Processes **2014**, *2*, 34-57; doi:10.3390/pr2010034

OPEN ACCESS

processes

ISSN 2227-9717

www.mdpi.com/journal/processes

Article

Model-Based Optimization of Scaffold Geometry and Operating Conditions of Radial Flow Packed-Bed Bioreactors for Therapeutic Applications

Danilo Donato, Ilaria E. De Napoli and Gerardo Catapano *

Department of Environmental, Territory and Chemical Engineering, University of Calabria, Via P. Bucci, 87030 Rende (CS), Italy; E-Mails: danilo.donato@unical.it (D.D.); ilaria.denapoli@gmail.com (I.E.D.N.)

* Author to whom correspondence should be addressed; E-Mail: gerardo.catapano@unical.it; Tel.: +39-0984-49-6666; Fax: +39-0984-49-6655.

Received: 18 September 2013; in revised form: 5 December 2013 / Accepted: 19 December 2013 / Published: 3 January 2014

Abstract: Radial flow perfusion of cell-seeded hollow cylindrical porous scaffolds may overcome the transport limitations of pure diffusion and direct axial perfusion in the realization of bioengineered substitutes of failing or missing tissues. Little has been reported on the optimization criteria of such bioreactors. A steady-state model was developed, combining convective and dispersive transport of dissolved oxygen with Michaelis-Menten cellular consumption kinetics. Dimensional analysis was used to combine more effectively geometric and operational variables in the dimensionless groups determining bioreactor performance. The effectiveness of cell oxygenation was expressed in terms of non-hypoxic fractional construct volume. The model permits the optimization of the geometry of hollow cylindrical constructs, and direction and magnitude of perfusion flow, to ensure cell oxygenation and culture at controlled oxygen concentration profiles. This may help engineer tissues suitable for therapeutic and drug screening purposes.

Keywords: bioreactor; model; oxygen; radial flow; tissue engineering; transport

---

Nomenclature

C	dissolved oxygen concentration in the construct [mol/m^3]
C_C	cell concentration in the construct [cells/m^3]

C_o	dissolved oxygen concentration in the feed [mol/m^3]
D	oxygen diffusion coefficient in water [m^2/s]
$Da_{rad,min} = V_{max}\delta_C/(v_oC_o)$	minimal radial Damköhler number in the construct [-]
D_C	oxygen dispersion coefficient in the construct [m^2/s]
$D_{eff} = D\cdot\varepsilon$	effective oxygen diffusion coefficient in the construct [m^2/s]
G	maximal cell-specific oxygen metabolic consumption rate [mol/(s cell)]
K_M	Michaelis constant for oxygen consumption [mol/m^3]
k	Darcy permeability of construct [m^2]
L	construct length [m]
NHy-FCV	non-hypoxic fractional construct volume [-]
P	pressure [Pa]
$Pe_{ax} = u_o\cdot L/D_C$	axial Peclet number [-]
$Pe_{rad,max} = v_o\cdot\delta_C/D_C$	maximal radial Peclet number [-]
Q	medium feed flow rate [m^3/s]
R_i	construct inner radius [m]
R_o	construct outer radius [m]
r	radial coordinate [m]
u	axial superficial velocity [m/s]
u_o	axial superficial velocity entering the construct [m/s]
$V_{max} = C_CG$	maximal metabolic consumption rate of oxygen [mol/(m^{3}s)]
v	radial velocity in construct [m/s]
v_o	maximal radial velocity in construct at r = R_i [m/s]
z	axial coordinate [m]

Greek Symbols

$\beta = K_M/C_o$	saturation parameter [-]
γ	perfusion flow direction parameter [-]
$\delta_C = R_o - R_i$	thickness of construct annular wall [m]
ε	construct porosity [-]
μ	medium viscosity [Pa·s]
$\varphi_C = \sqrt{(V_{max}\cdot\delta_C/(D_C\cdot C_o))}$	Thiele modulus in construct perfused with medium [-]
$\varphi_D = \sqrt{(V_{max}\cdot\delta_C/(D_{eff}\cdot C_o))}$	Thiele modulus in construct under static operation [-]
τ	average shear stress in construct [Pa]

Superscripts and Subscripts

ax	axial
C	construct
max	maximal
rad	radial
*	dimensionless

1. Introduction

In recent years, the scarcity of donor tissue to replace the mechanical or metabolic functions of missing or failing tissue has prompted the search for alternative treatments [1]. An interesting alternative to tissue replacement with artificial grafts and to animal models for *in vitro* drug screening is to engineer biological substitutes of human tissue by seeding isolated autologous cells in three-dimensional (3D) porous scaffolds and by guiding cell re-organization and differentiation in bioreactors in which cells are subject to physiological mechanical and biochemical cues. In the repair of large bone defects, the presence of autologous cells could eliminate rejection of allo- or xenografts and could enhance graft osteointegration as compared to artificial bone grafts [2]. In the extracorporeal assist to liver failure patients, treatments based on bioreactors using engineered liver tissue could provide the patient with more liver-specific functions (virtually all of them) than non-specific artificial treatments and bioreactors using immortalized cell lines or enzymes [3].

An important step in the realization of clinical-scale engineered tissue is the construct culture in bioreactors designed and operated in such a way to guide cell re-organization and differentiation as in the natural tissue. Cell culture in the presence of controlled physiological concentrations and supply of nutrients and dissolved oxygen is a basic bioreactor requirement to ensure cell survival and to make cells differentiate to a given phenotype. In particular, oxygen is acknowledged a major limiting role to the development of engineered substitutes mimicking natural tissues [4–8]. Metabolic soluble species are generally supplied in the culture medium. To reach the cells anywhere in the construct, such solutes have to be transported external to the construct (*i.e.*, from the medium bulk to the construct outer surface) and inside the construct (*i.e.*, from its outer surface to the innermost regions) across the cell mass [9]. Pure diffusive transport in static bioreactors ensures dissolved oxygen and nutrients supply only to a distance about 100 μm away from the construct outer surface, it subjects cells to oxygen and nutrients concentrations largely varying in space (e.g., across the construct), and ultimately limits the realization of clinical-scale 3D cell constructs [10–14]. To minimize the diffusive limitations to external solute transport, bioreactors have been proposed in which some degree of external convection is superimposed over pure diffusion by perfusing the medium around or along the construct. Radial medium perfusion along two-dimensional (2D) cultures of liver cells in a gel sandwich adherent to glass discs [15] or constrained between microporous membranes encased in a rigid frame [16] permits the design of more compact bioreactors than the typical flasks or dishes. Medium convection around 3D porous constructs in spinner flasks and rotating wall vessel bioreactors has been reported to improve cell distribution and viability with respect to static bioreactors but has not been shown to permit adequate oxygen and nutrients supply to cells deep into the construct and adequate expression of cell differentiation markers [17–19]. Medium supplementation with carriers reversibly binding oxygen (e.g., cross-linked hemoglobins or perfluorocarbons) has also been proposed to mimic the oxygen storage function of hemoglobin in the red blood cells and overcome the low solubility of oxygen in aqueous media [20,21]. The inclusion of porous hydrophobic microspheres in 3D collagen gel constructs has been shown to enhance oxygen diffusive transport, and increase the oxygen penetration depth, into the construct and hepatocyte functions by promoting some degree of local natural convection at the gel interface with the microspheres [22,23]. Direct axial perfusion of 3D porous constructs with medium in axial-flow packed bed bioreactors (aPBBs) uses convection to

enhance oxygen and nutrients transport to cells internal to the construct [24–27]. However, at low axial superficial velocity the dissolved oxygen and nutrients concentrations may steeply decrease towards the end of the construct leading to poor cell nourishment and causing the formation of a necrotic end zone [28,29]. Cell perfusion at high axial superficial velocity to keep cells viable and differentiated anywhere in the construct may cause cell wash-out [30].

Radial perfusion with medium of cells seeded in 3D cylindrical porous scaffolds with a coaxial hollow cavity has been proposed to overcome the transport limitations of pure diffusive operation and direct axial perfusion [31]. Similar to axial perfusion, superimposition of convection to pure diffusion should enhance solute transport to cells. Radially perfused hollow constructs would also feature a larger cross-sectional area for solute transport and shorter solute transport path-length than axially perfused constructs. Hence, cell constructs could be cultured in radial-flow packed-bed bioreactors (rPBBs) at lower pressure drop and lower superficial velocity (hence lower shear stresses) than aPBBs and still enable cell culture under smoother and more controllable dissolved oxygen and nutrients concentration gradients in the direction of medium perfusion [32]. This is a very interesting feature to control cell pericellular environment and to guide cell differentiation when realizing biological tissue substitutes for implantation or for the *in vitro* toxicity screening of new drugs [33].

In spite of these interesting features, only a few reports have been published on the culture of human cells seeded in 3D porous scaffolds in radial-flow packed-bed bioreactors for therapeutic applications. Inward radial perfusion of 3D constructs in rPBBs has been shown to promote cell proliferation to a greater extent than static operation in the culture of NIH/3T3 cells in poly(L)lactic acid porous scaffolds [34], and of sheep mesenchymal stem cells [35] and MG63 osteoblast-like cells [36] in β-tricalcium phosphate (β-TCP) porous scaffolds. In the development of a bioartificial liver, inward radial perfusion culture in rPBBs has been reported to maintain in an active metabolic state high concentrations of human liver cancer cells FLC-7 [37], HepG2 cells [38], and porcine hepatocytes [39] in small-scale constructs, and of porcine primary hepatocytes in clinical-scale constructs [40,41]. The co-culture in rPBBs of immortalized [42] and primary fetal hepatocytes and non-parenchymal cells [43] in a 3D porous scaffold perfused inwards has been reported to promote the partial organization of cells in a liver-like architecture with sinusoid-like lumen structures and sustained liver-specific functions for a week. Olivier *et al.* [36] reported that inward medium perfusion enhances MG63 cell proliferation and metabolic activity in β-TCP porous scaffolds to a greater extent than outward medium perfusion.

In the absence of thorough experimental information, the peculiar features of rPBBs could be exploited with the help of mathematical models of momentum and solute transport across the construct. In this paper reference is mainly made to the few models proposed for mammalian cell culture in rPBBs because they account for some typical cell features, such as the sensitivity of their metabolism to the culture environment (e.g., pericellular dissolved oxygen and nutrients concentration, shear stress, pressure), and the fact that some cell types proliferate during culture thus changing both the geometry of the flow channel and the conditions under which the bioreactor is operated, among others. All models propose a pseudo-homogeneous description of transport across the construct, and neglect transport in the inner hollow cavity and the peripheral annular space. Tharakan and Chau [44] proposed a steady-state transport model of the limiting metabolic substrate and the products across an annular bed of mammalian cells perfused outwards with medium for the production of monoclonal

antibody. The model accounts for dispersive and convective solute radial transport across the cell construct, for substrate consumption in terms of the Monod kinetics and for the possible presence of semipermeable membranes in the cell mass, albeit in lumped fashion. The model was used to investigate the effect of the dimensionless radial superficial velocity, the dimensionless construct thickness, and the cell metabolic activity on the substrate conversion to products and their distribution across the cell construct. Cima *et al*. [45] described the steady-state transport by diffusion and convection of dissolved oxygen and nutrients across an annular bed of cells seeded in the thin gap between two concentric thick-walled microporous hollow fiber membranes. Dimensionless analytic expressions for the dissolved oxygen and nutrients concentrations across the cell mass have been reported for zero-th order cellular consumption kinetics and for uniform solute concentrations in the inner fiber lumen and outside the outer fiber wall, equal to each other. The model was used to investigate the effect of the dimensionless radial superficial velocity and solute consumption rate on the dissolved oxygen and nutrients concentrations across the cell mass for a given hollow fiber membranes geometry, outward medium perfusion flow, and cells with low metabolic requirements. Böhmann *et al*. [46] developed and experimentally validated a lumped parameter model describing radial perfusion and metabolic consumption of dissolved oxygen across a 35 mm thick annular bed of SIRAN® macroporous beads wrapped in a dialysis membrane in which hybridoma cells were cultured. The model was used to investigate the influence of the concentration of low-molecular weight solutes, freely permeable across the membrane, and high molecular weight solutes, retained in the bed, on long-term monoclonal antibody production. The model enabled the bioreactor scale-up from a 0.1 L to a 5 L bed volume [47]. To the best of the authors' knowledge a systematic analysis of the influence on bioreactor performance of dimensionless parameters accounting for the annular bed geometry and shape, a concentration-dependent solute consumption kinetics, and the direction of the perfusion flow under the constraints typical of therapeutic applications (e.g., the replacement of tissue structure or functions in therapeutic treatments or in the *in vitro* drug screening) has not been reported yet. This hinders recognition of the most relevant parameters determining the rPBB behavior and the understanding of the interplay among such parameters, and makes it difficult to optimize bioreactor design and operation for a given therapeutic objective.

In this paper, it is proposed a model-based reference framework aimed to optimize scaffold geometry and operating conditions (*i.e.*, direction and superficial velocity of the perfusing medium) of convection-enhanced rPBBs for therapeutic applications. The framework relies on a pseudo-homogeneous model based on the Darcy and the convection-dispersion-reaction equation to describe the pseudo steady-state transport of momentum and dissolved oxygen in annular porous constructs of varying geometry, which are perfused with medium flowing in different directions and in which human cells consuming oxygen according to Michaelis-Menten kinetics are cultured at varying concentrations. Dimensional analysis is used to identify the dimensionless groups determining the bioreactor performance expressed in terms of a more apt parameter to therapeutic applications. The aim is to provide the bioreactor designer with a tool for helping in the optimization of design and operation of convection-enhanced rPBBs and for enabling control of the pericellular concentrations of dissolved oxygen, but also of low molecular weight nutrients and biochemical cues, to prevent cell starvation, to guide their differentiation towards a given phenotype, and to assess drug toxicity under known environmental conditions and cell state.

2. Materials and Methods

2.1. Model Development

2.1.1. Convection-Enhanced Transport Model of rPBB

A model was developed to describe the transport of momentum and low molecular weight solutes in convection-enhanced radial packed-bed bioreactors. The attention was focused on oxygen for its importance to cell metabolism [4–8]. Schemes of an rPBB with opposite perfusion flows are reported in Figure 1. The bioreactor consists of a cylindrical chamber equipped with inlet and outlet fittings in which it is located a 3D cylindrical porous scaffold of length L, outer radius R_o, and porosity ε, with a coaxial hollow cavity of radius R_i. Human cells are seeded and cultured at a concentration C_C in the pores of the construct annular wall of thickness δ_C. Medium of viscosity μ carrying oxygen at a concentration C_o is fed to the bioreactor at a flow rate Q and continuously flows radially across the construct from the outer peripheral annular space towards the inner hollow cavity (*i.e.*, inwards), as shown in Figure 1a, or from the inner hollow cavity towards the outer peripheral annular space (*i.e.*, outwards), as shown in Figure 1b, at a maximal superficial velocity v_o at the inner construct surface (*i.e.*, $r = R_i$). In the inner hollow cavity and the peripheral annular space medium is assumed to flow axially in opposite directions and is assumed well-mixed (*i.e.*, solute concentration is uniform throughout). The flow configurations considered are often referred to as CP-π flow (or centripetal) (Figure 1a) or CF-π flow (or centrifugal) (Figure 1b) [48]. The term π-flow indicates that medium flow directions in the inner hollow cavity and the peripheral annular space are opposite. Dissolved oxygen is carried by the medium into the construct where it is transported to the cells by convection (*i.e.*, associated to the net medium flow) and dispersion with a dispersion coefficient D_C (*i.e.*, transport is promoted by a concentration gradient in the presence of the flowing medium), and it is metabolized by the cells. At low medium superficial velocity across the construct, the concentration gradient-driven oxygen transport occurs mainly by diffusion [49]. At high medium superficial velocity, the mixing generated by the medium flowing across the porous scaffold becomes important and the concentration gradient-driven oxygen transport is mainly dispersive [49]. The conservation equations governing the rPBB performance were obtained under the following assumptions:

1. axial symmetry;
2. steady-state conditions;
3. incompressible fluid;
4. isothermal conditions;
5. transport in the construct is described according to a pseudo-homogeneous approach;
6. construct is described as an isotropic porous medium with Darcy permeability k;
7. uniform cell distribution C_C;
8. no cell lysis or apoptosis;
9. solute concentration in the construct does not vary along the axial and angular coordinates;
10. momentum transport in the construct is described according to the Darcy equation;
11. dissolved oxygen is transported across the construct by convection and dispersion;

12. cells consume oxygen according to Michaelis-Menten kinetics, with a maximal cell-specific consumption rate G and a Michaelis constant K_M.

Under these assumptions, upon introducing the following non-dimensional coordinates and variables

$$r^* = \frac{r}{R_i};\ v^* = \frac{v}{v_o};\ P^* = \frac{P}{v_o \mu L / R_i^2};\ C^* = \frac{C}{C_o};\ \beta = \frac{K_M}{C_o} \tag{1}$$

the governing conservation equations in the construct may be re-arranged in dimensionless form to give:
continuity equation

$$v^* = \frac{1}{r^*} \tag{2}$$

momentum conservation (Darcy equation)

$$v^* = -\gamma \frac{kL}{R_i^3} \frac{dP^*}{dr^*} \tag{3}$$

mass conservation

$$Pe_{rad,\max} \frac{R_i}{\delta_C} \left(v^* \frac{dC^*}{dr^*} \right) = \frac{1}{r^*} \frac{d}{dr^*} \left(r^* \frac{dC^*}{dr^*} \right) - \gamma\, \varphi_C{}^2 \frac{R_i^2}{\delta_C{}^2} \frac{C^*}{\beta + C^*} \tag{4}$$

where $\gamma = 1$ in the case of outward flow, and $\gamma = -1$ in the case of inward flow. Equation (3) is subject to the boundary condition stating that the outlet pressure equals atmospheric pressure, as follows:
B.C.1

$$\textit{outward flow}\ (\gamma = 1) \qquad r^* = 1 + \frac{\delta_C}{R_i} \qquad P^* = 0; \tag{5a}$$

$$\textit{inward flow}\ (\gamma = -1) \qquad r^* = 1 \qquad P^* = 0; \tag{5b}$$

Equation (4) is subject to two boundary conditions, of which B.C.2 states the continuity of solute flux at the entrance to the construct in terms of Danckwert's condition, and B.C.3 states the continuity of fluxes across the outer construct surface when solute concentration does not change any further once the medium leaves the construct, as follows:
B.C.2

$$\textit{outward flow}\ (\gamma = 1) \qquad r^* = 1 \qquad 1 = C^* - \frac{1}{Pe_{rad,\max}} \frac{\delta_C}{R_i} \frac{dC^*}{dr^*} \tag{6a}$$

$$\textit{inward flow}\ (\gamma = -1) \qquad r^* = 1 + \frac{\delta_C}{R_i} \qquad 1 = C^* - \frac{1}{Pe_{rad,\max}} \frac{\delta_C}{R_i} \left(1 + \frac{\delta_C}{R_i} \right) \frac{dC^*}{dr^*} \tag{6b}$$

B.C.3

$$\textit{outward flow}\ (\gamma = 1) \qquad r^* = 1 + \frac{\delta_C}{R_i} \qquad \frac{dC^*}{dr^*} = 0 \tag{7a}$$

$$\textit{inward flow}\ (\gamma = -1) \qquad r^* = 1 \qquad \frac{dC^*}{dr^*} = 0 \tag{7b}$$

when $Pe_{rad,\max} >> 1$, Equations (6a,b) states that solute concentration in the stream entering the construct equals that in the feed.

Figure 1. Scheme of radial flow packed-bed bioreactors (rPBBs) with opposite perfusion flows across the annular construct wall: (**a**) inward flow; (**b**) outward flow.

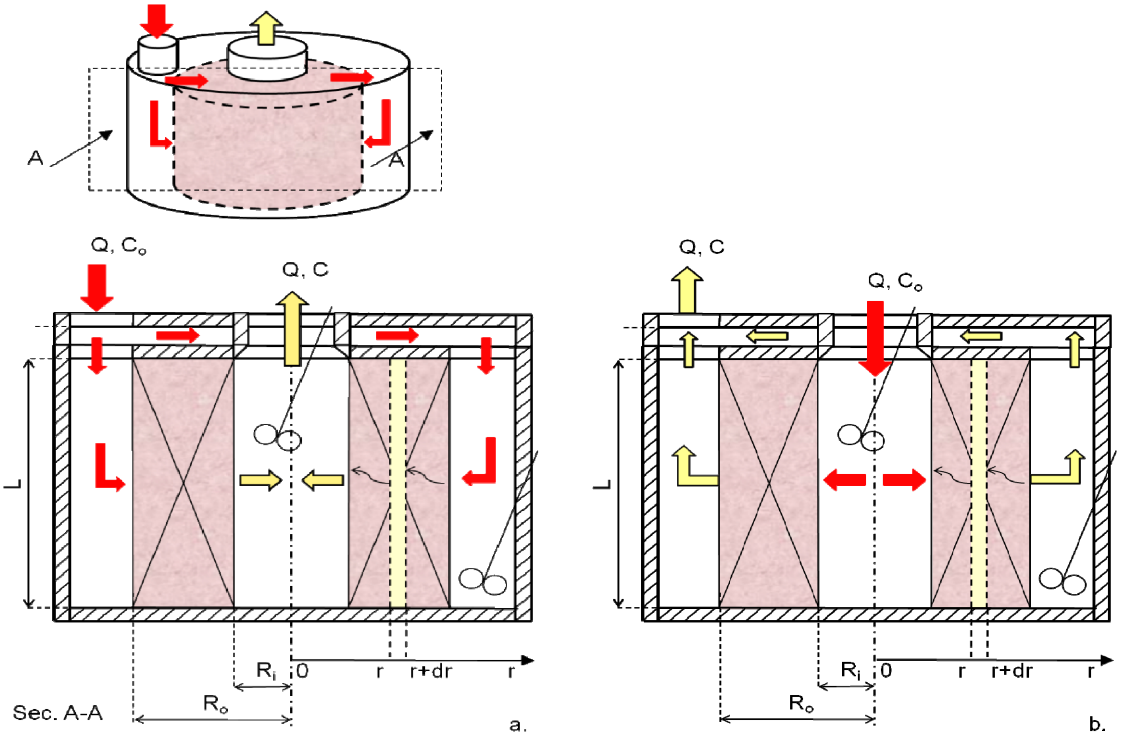

2.1.2. Diffusion-Limited Transport Model of rPBB

For the sake of comparison, a diffusion-limited model of solute transport in the rPBB was also developed. In this case, the construct is assumed to be dipped and held suspended in medium carrying oxygen at a concentration C_o in a reservoir and medium has unhindered access to the hollow cavity. Under the same assumptions as in the convection-enhanced transport model, but for the fact that oxygen transport occurs only by diffusion with an effective diffusion coefficient D_{eff}, and for the same non-dimensional coordinates and variables as in Equation (1), the governing mass conservation equation in the construct may be re-arranged in dimensionless form to give:

$$\frac{1}{r^*}\frac{\mathrm{d}}{\mathrm{d}r^*}\left(r^*\frac{\mathrm{d}C^*}{\mathrm{d}r^*}\right)=\varphi_D{}^2\frac{R_i^2}{\delta_C{}^2}\frac{C^*}{\beta+C^*} \tag{8}$$

which is subject to two boundary conditions stating that both the inner and the outer construct surfaces are exposed to the same dissolved oxygen concentration in medium C_o (*i.e.*, well mixed reservoir):

B.C.1

$$r^*=1 \qquad C^*=1 \tag{9a}$$

B.C.2

$$r^*=1+\frac{\delta_C}{R_i} \qquad C^*=1 \tag{9b}$$

2.1.3. Convection-Enhanced Transport Model of aPBB

To compare the rPBB performance to that of an aPBB, reference was made to the dimensionless design equations of aPBBs in which medium carrying oxygen at a concentration C_o perfuses at an axial superficial velocity u_o a cylindrical construct of length L and radius R_i, as in [50]. Under the same assumptions as in the convection-enhanced transport model of rPBB, and for the same non-dimensional coordinates and variables as in Equation (1) but for $z^* = z/L$, the governing mass conservation equation in the construct may be re-arranged in dimensionless form to give:

momentum conservation (Darcy equation)

$$u^* = -\frac{k}{R_i^2}\frac{dP^*}{dz^*} \tag{10}$$

mass conservation

$$Pe_{ax}\, u^*\left(\frac{dC^*}{dz^*}\right) = \frac{d^2C^*}{dz^{*2}} - \varphi_C{}^2\frac{C^*}{\beta + C^*} \tag{11}$$

Equation (10) is subject to the boundary condition stating that the outlet pressure equals atmospheric pressure, as follows:

B.C.1

$$z^* = 1 \qquad P^* = 0 \tag{12}$$

Equation (11) is subject to two boundary conditions of which B.C.2 states the continuity of solute flux at the entrance to the construct in terms of Danckwert's condition, and B.C.3 the continuity of fluxes across the outer construct surface when solute concentration does not change any further once the medium leaves the construct, as follows:

B.C.2

$$z^* = 0 \qquad 1 = C^* - \frac{1}{Pe_{ax}}\frac{dC^*}{dz^*} \tag{13a}$$

B.C.3

$$z^* = 1 \qquad \frac{dC^*}{dz^*} = 0 \tag{13b}$$

2.2. Dimensionless Groups

2.2.1. Convection-Enhanced Transport Model of rPBB

Analysis of dimensionless Equations (1)–(7) shows that the rPBB performance is determined by the six dimensionless groups reported in Table 1. The physical interpretation of most of these dimensionless groups is well established [51]. The dimensionless group $k\,L/R_i^3$ may be interpreted as the dimensionless Darcy permeability of the construct and provides information about the radial pressure drop across the construct at a given flow rate. The higher its value, the lower the radial pressure drop across the construct. The construct inner radius-to-wall thickness ratio, R_i/δ_C, accounts for the construct curvature. The higher the inner radius or the thinner the thickness of the annular wall,

the more negligible the construct curvature. The maximal radial Peclet number, $Pe_{rad,max}$, compares the maximal rate of solute transport in the construct by convection to dispersion. The higher its value, the higher the importance of convection to solute transport as compared to dispersion. The Thiele modulus compares the maximal zero-th order solute consumption rate, $V_{max} = C_C \cdot G$, to the maximal rate of dispersive solute transport, $C_o\ D_C/\delta_C^2$. High Thiele moduli may be associated with high cell concentrations, C_C, or high cell-specific metabolic consumption rates, G. The saturation parameter β provides information on the extent to which the consumption kinetics differs from the zero-th order. The higher its value, the closer the kinetics to the first order.

Table 1. Dimensionless groups determining the rPBB performance.

Group Definition	Description
1. γ	perfusion flow direction parameter
2. $k\ L/R_i^3$	dimensionless Darcy permeability of construct
3. R_i/δ_C	inner radius-to-thickness ratio of the construct
4. $v_o\ \delta_C/D_C$	maximal radial Peclet number, $Pe_{rad,max}$
5. $\sqrt{(V_{max}\delta_C^2/(D_C\ C_o))}$	Thiele modulus, φ_C
6. K_M/C_o	saturation parameter, β

2.2.2. Diffusion-Limited Transport Model of rPBB

Analysis of dimensionless Equations (8) and (9) shows that under diffusion-limited operation, the performance of the rPBB is determined only by the construct curvature, R_i/δ_C, the Thiele modulus $\varphi_D = \sqrt{(V_{max}\ \delta_C^2/(D_{eff}\ C_o))}$ and the saturation parameter $\beta = K_M/C_o$.

2.2.3. Convection-Enhanced Transport Model of rPBB

Analysis of dimensionless Equations (10)–(13) shows that the dimensionless groups determining the performance of an axial-flow packed bed bioreactor are the dimensionless Darcy permeability of the construct, k/R_i^2, the axial Peclet number, $Pe_{ax} = u_o\ L/D_C$, the Thiele modulus $\varphi_C = \sqrt{(V_{max}\ L^2/(D_C\ C_o))}$ and the saturation parameter $\beta = K_M/C_o$.

2.3. Computational Methods

The resulting set of governing equations for a convection-enhanced or a diffusion-limited rPBB, and for an aPBB, was integrated numerically with the commercial Finite Element Method (FEM) code Comsol Multiphysics (Comsol Inc., Burlington, MA, USA). An optimal non-uniform mesh with more than 20,000 rectangular elements, finer at the construct inner and outer surfaces, was generally used to describe the spatial domain. Model-predicted spatial profiles of superficial velocity, pressure and dissolved oxygen concentration were obtained for values of the model parameters and dimensionless groups representative of those used in experiments in which rPBBs were used, or typically reported or of interest for therapeutic applications, as reported in Tables 2 and 3 unless otherwise stated. In particular, the effective diffusivity of oxygen, D_{eff}, was estimated according to [50] by multiplying that in water at 37 °C [52] by a construct porosity $\varepsilon = 0.7$, typical of the 3D porous scaffolds used in rPBBs [35,36]. The dispersion coefficient for oxygen in the construct was estimated by adjusting the

diffusivity according to the correlations for liquids in [49] for the value of the maximal radial superficial velocity, v_o. The value of v_o was set equal to 1.98×10^{-4} m/s throughout, consistent with the values used in the few culture experiments reported for rPBBs with small-scale constructs seeded with human cells [35,36].

Table 2. Dimensionless group values used for model predictions, unless otherwise stated.

Dimensionless Group	Values
1. perfusion flow direction parameter, γ	−1 (inwards), 1 (outwards)
2. dimensionless Darcy permeability of construct, $k\,L/R_i^3$	2.24×10^{-10}–2.24×10^{-4}
3. construct curvature, R_i/δ_C	0.1–10
4. maximal radial Peclet number, $Pe_{rad,max}$	49
5. Thiele modulus, φ_C or φ_D	1–20
6. saturation parameter, β	0.019

Table 3. Model parameter values used for model predictions, unless otherwise stated.

Symbol	Model Parameter	Value	Units	Reference
C_o	oxygen inlet concentration	0.216	mol/m^3	[53]
D	oxygen diffusivity in water	2.64×10^{-9}	m^2/s	[52]
D_{eff}	effective oxygen diffusivity in the construct	1.85×10^{-9}	m^2/s	[50]
D_C	oxygen dispersivity in the construct	2×10^{-8}	m^2/s	[49]
K_M	oxygen Michaelis constant	4.05×10^{-3}	mol/m^3	[54]
k	Darcy permeability of construct	1.4×10^{-13}	m^2	[55]
L	scaffold length	0.2	m	
v_o	maximal inlet superficial velocity	1.98×10^{-4}	m/s	[36]
δ_C	scaffold thickness	0.005	m	[36]
μ	medium viscosity	6.92×10^{-4}	Pa s	[53]

Although the spatial dissolved oxygen concentration profiles are essential to assess the actual pericellular culture conditions, a more helpful approach to the first decisional phases of design is to condense bioreactor performance in one parameter only, and to analyze the influence of the most relevant dimensionless groups on this performance parameter. With respect to oxygen, the basic requirement for cell survival is that cells should be supplied with physiological amounts of oxygen and should be cultured at physiological dissolved oxygen concentrations anywhere in the construct. To this purpose, an alternative performance parameter was introduced that was deemed more significant to bioreactor designers for therapeutic applications. It provides information on the volume fraction of the construct in which cells are exposed to physiological dissolved oxygen concentrations, and was termed the non-hypoxic fractional construct volume (NHy-FCV). In this work, the minimal value for physiological oxygen concentrations was set equal to 2×10^{-2} mM, a typical threshold for mammalian cells [56].

3. Results and Discussion

Radial-flow packed bed bioreactors have distinctive features that make them interesting for therapeutic applications. Their structure resembles the architecture of long bones (e.g., the femur shaft) [57]

and the medium perfusion pattern is similar to blood in the liver lobule [58], when the construct is perfused inwards. Radial perfusion enhances solute transport to cells with respect to pure diffusion. Radially perfused hollow cylindrical constructs feature also a larger cross-sectional area and a shorter path-length for solute transport than axially perfused constructs. In this paper, a model reference framework is proposed to help designers of rPBBs optimize their geometry and operation to meet given therapeutic requirements. The framework is based on the model described by Equations (1)–(9) in which the pseudo steady-state transport of momentum and dissolved oxygen across an annular cell-seeded construct is described according to the Darcy and the dispersion-convection-reaction equation, respectively. The dimensionless groups determining the actual dissolved oxygen concentration profile in the construct and the performance of the rPBB were obtained by dimensional analysis of Equations (1)–(9) and are shown in Table 1. The pseudo steady-state assumption is not a limitation to the use of the model. In fact, the large difference in the time scale typical of bioreactor dynamics (of the order of the minute) and of the kinetics of cell growth (of the order of the day), makes it possible to use the model for investigating bioreactor performance as cells proliferate and/or secrete an own ECM by adjusting the dimensionless groups values to the maturation of the cell construct. Another important assumption in the model development is that medium flows at uniform superficial radial velocity along the bioreactor length. In fact, maldistribution of radial velocity has been reported to have more influence on the performance of radial-flow packed bed reactors for industrial applications than other parameters, such as the flow direction [59]. In the use of rPBBs for human cell culture, a non-uniform superficial radial velocity would cause a non-uniform supply of dissolved oxygen, nutrients and biochemical cues to cells that, during culture, might yield a non-uniform cell distribution in the construct as an effect of poor cell proliferation or cell necrosis in the poorly perfused regions of the construct. As tissue matures, this would cause the Darcy permeability of the construct to decrease non-uniformly thus worsening even further the radial flow maldistribution and its effects. As Figure 1 shows, in the model development reference was made to rPBBs in which the directions of axial flow in the inner hollow cavity and the outer peripheral annular space are opposite, *i.e.*, a π-flow type bioreactor configuration, to make it more likely that the actual radial superficial velocity be uniformly distributed along the bioreactor length under actual operation. In fact, if the frictional pressure drop is negligible in the inner hollow cavity and the outer peripheral annular space, independent of the flow direction, the axial pressure profiles in these regions develop in such a way to maintain a constant radial pressure drop across the construct [48].

The scarcity of experimental data for human cell culture in convection-enhanced rPBBs and the difficult procurement of detailed information on the conditions and geometry used made it awkward to validate the model. For these reasons, model goodness was assessed by comparing the model-predicted dissolved oxygen concentration profiles across the annular constructs to those predicted by Cima *et al*. [45] and the model-predicted glucose consumption, to that reported by Olivier *et al*. [36] for the culture of osteosarcoma cells in an rPBB perfused with medium both inwards and outwards, as shown in Figure 2. In the latter case, the rPBB was assumed to be connected in closed loop to a completely mixed reservoir, and its dynamics was neglected with respect to the reservoir on the account of its small volume. Glucose consumption was estimated from the model-predicted decrease of glucose concentration in the reservoir after 24 h. Figure 2a shows that the predictions of the model presented in this paper were in good agreement with those reported by Cima *et al*., for the

geometry and the operating conditions used therein, *i.e.*, zero-th order consumption kinetics, Thiele moduli typical of cells with low metabolic requirements, and exposure of the construct inner and outer surfaces to equal dissolved oxygen concentrations [45]. Figure 2b shows that the model effectively predicted also the experimental results reported by Olivier *et al*., for the culture of osteosarcoma cells in an rPBB [36]. In this case, the cell-specific glucose consumption rate was estimated with the diffusion-limited transport model as that best fitting the experimental data reported for static culture in the rPBB. When medium was perfused outwards, the decreased cell concentrations that were observed by Olivier *et al*. in the construct, likely as an effect of cell wash-out, were taken into account.

Figure 2. Comparison of model-predicted low molecular weight substrate concentrations to: (**a**) the theoretical predictions for dissolved oxygen of Cima *et al*. [45]; (**b**) the experimental data for glucose consumption of Olivier *et al*. [36]. Predictions obtained for the following parameter values: (**a**) $\gamma = 1$, $R_i/\delta_C = 1.49$, $Pe_{rad,max} = 0.67$, $k\,L/R_i^3 = 1.5 \times 10^{-2}$, $\varphi_C = 1.16$ (●) and 1.34 (■); (**b**) $R_i/\delta_C = 0.4$, $Pe_{rad,max} = 1071$, $k\,L/R_i^3 = 2.5 \times 10^{-7}$, $\varphi_C = 0.82-0.93$, $\beta = 0.02$, for perfusion inwards $\gamma = 1$ (♦), outwards $\gamma = -1$ (■), or static operation (x).

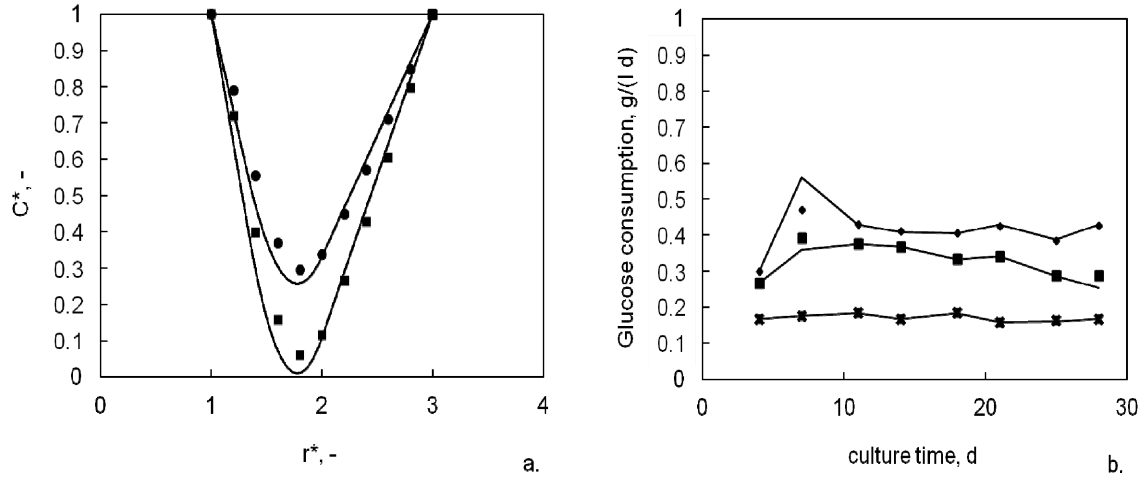

Model predictions show the convenient characteristics of radial-flow packed bed bioreactors as compared to static operation and axial-flow packed bed bioreactors in the culture of cell-seeded constructs. Figure 3 shows that radial perfusion in an rPBB may yield better oxygen supply to cells anywhere in the construct and more uniform pericellular dissolved oxygen concentrations than static operation. In spite of the fact that under static operation oxygen is supplied to cells through both the inner and the outer construct surfaces, when transport is diffusion-limited the dissolved oxygen concentration steeply decreases towards the innermost regions of the annular construct. Oxygen depletion gets worse when highly concentrated cells with high metabolic requirements are cultured, *i.e.*, as the Thiele modulus increases. Figure 3a,b shows that under static operation for $V_{max} = 1.76 \times 10^{-9}$ mol/(mL s) cells would be cultured under anoxic conditions in about 65% of the construct volume. This could be the case of osteoblasts consuming oxygen at $G = 5.5 \times 10^{-17}$ mol/(s cell) [60] cultured in a 3D porous hollow cylindrical scaffold at a concentration of $C_C = 3.2 \times 10^7$ cells/mL [26]. When the same construct is radially perfused with medium at $Pe_{rad,max} = 49$, independent of the direction of the perfusion flow, the radial dissolved oxygen

concentration profile is about uniform across the construct at the same value as in the feed as long as the cell-specific oxygen consumption rate and cell concentration yields V_{max} up to *ca*. 1.8×10^{-10} mol/(s mL). Independent of the flow direction, at higher Thiele moduli the dissolved oxygen concentration smoothly decreases along the direction of medium perfusion. Figure 3a,b shows that for $V_{max} = 1.76 \times 10^{-9}$ mol/(s mL) the minimal dissolved oxygen concentration nowhere gets below ca. 50% of that in the feed. Such a remarkable transport enhancement may be attributed directly to convection, but also to the convection-related increase of the dispersion coefficient.

Figure 3. Dimensionless radial oxygen radial concentration profiles at varying maximal oxygen consumption rates V_{max}: (i) 1.76×10^{-10} mol/(s mL); (ii) 8.8×10^{-10} mol/(s mL); (iii) 1.76×10^{-9} mol/(s mL) for cells cultured in a hollow cylindrical construct in an rPBB radially perfused with medium (solid lines) (**a**) outward or (**b**) inwards, or (dashed lines) statically operated. Parameter values: $R_i/\delta_C = 0.4$, $Pe_{rad,max} = 49$. Other parameters are as in Tables 2 and 3.

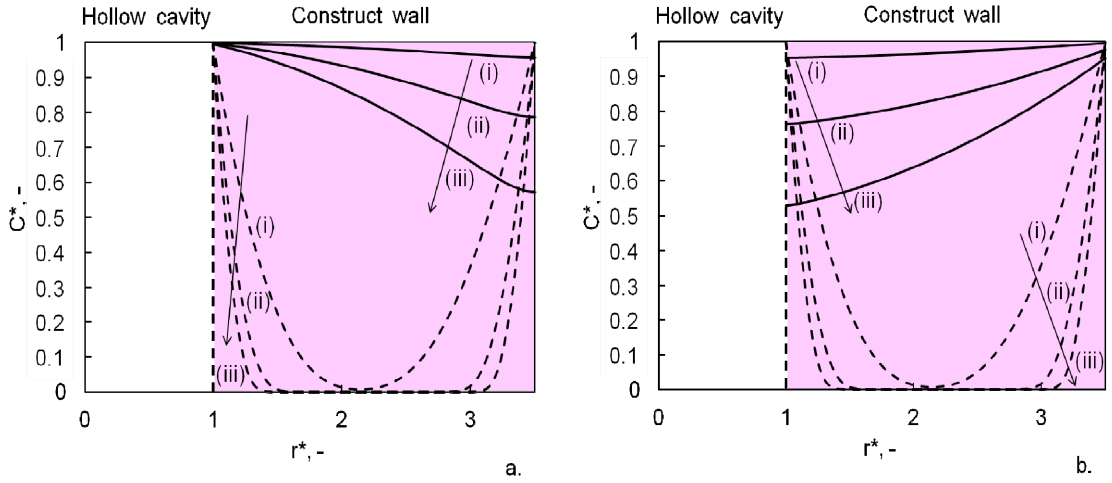

The performance of an rPBB was compared to that of an aPBB for the case of the bioengineering of a clinical-scale long bone graft (e.g., a femur shaft) or of a bioreactor for a bioartificial liver (BAL), under the constraint that the construct length and volume, and the maximal superficial velocity be equal to the aPBB. For the superficial velocity this means that $v_o = u_o$. In the case of the aPBB, the bioengineered femur shaft was approximated with a cylindrical porous construct 40 cm long and 3.5 cm in diameter, similar in size to the human femur shaft [57], and the bioreactor for BAL was assumed to be based on a cylindrical porous construct 20 cm long and 3 cm in diameter so as to be easily fitted in the housing of some clinical-scale BAL bioreactors proposed in the last years [19]. In either case, the rPBB was assumed to be equipped with a cylindrical construct of equal length and volume with an inner hollow cavity of radius $R_i = 5$ mm. For the bone graft, the constructs were assumed to be seeded with 10^7 osteoblasts/mL consuming oxygen at 5.5×10^{-17} mol/(cell s) [60]. For the liver graft, it was considered the possibility that the constructs are seeded with either hepatocytes or HepG2 cells, consuming oxygen at 9×10^{-16} mol/(cell s) [61] or 6.62×10^{-17} mol/(cell s) [62], respectively. Radial medium perfusion across the construct generally yields dissolved oxygen concentration profiles, which decrease more smoothly in the direction of medium perfusion than in aPBBs. In the case of the bioengineered long bone graft, Figure 4a shows that in an aPBB

the dissolved oxygen concentration steeply decreases away from the entrance. This results in a non-hypoxic fractional construct volume of only NHy-FCV = 0.18 and causes cells to be cultured under anoxic conditions in about 78% of the construct volume. Figure 4b shows that in an rPBB the dissolved oxygen concentration in the construct decreases more smoothly in the direction of the perfusion flow and it is nowhere below 62% of the feed, largely exceeding the set physiological threshold value. Similar results were obtained in the case of bioreactors for BAL seeded with the HepG2 immortalized cell line (data not shown). Oxygen depletion was much more severe in bioreactors seeded with primary hepatocytes causing cells to be cultured under anoxic conditions in more than 60% of the construct volume. However, in the rPBB the well oxygenated fractional construct volume was about fifteen fold higher than in the aPBB (31% *vs*. 2%, respectively). The transport enhancement in the rPBB may be attributed to the shorter oxygen transport path-length than the aPBB (*i.e.*, the construct annular thickness *vs*. length) that apparently more than compensates for the fact that the axial Peclet number in the aPBB is more than one order of magnitude higher than the maximal radial Peclet number in the rPBB. Bioreactor performance was compared at $v_o = u_o = 1.98 \times 10^{-4}$ m/s because this would guarantee that cells are not damaged by shear stresses. In fact, if the average shear stress acting on cells for medium perfusion in the construct is estimated according to [63], as follows:

$$\tau = \frac{\mu \ v_o}{\sqrt{k}} \tag{14}$$

it may be estimated that $\tau = 0.35$ Pa in both bioreactors. This is below the reported range of laminar shear stress at which adherent cells are removed from surfaces [64]. However, the maximal pressure drop across the axially perfused construct is about two orders of magnitude higher than in the radially perfused construct which may compress or even crush soft scaffolds and cause mechanical damage to cells or cell wash-out. Increasing u_o in the aPBB to obtain a smoother axial dissolved oxygen concentration profile would cause an even greater increase of the axial pressure drop that may worsen these effects.

Figure 4. Dimensionless oxygen concentrations in a 3D porous bone construct perfused with medium: (**a**) axially ($Pe_{ax} = 3910$); (**b**) radially outwards ($Pe_{rad,max} = 129$, $R_i/\delta_C = 0.38$, $\gamma = 1$). Parameter values: $C_C = 10^7$ cell/mL, $G = 5.5 \times 10^{-17}$ mol/(s·cell), $L = 40$ cm. Other parameters are as in Tables 2 and 3.

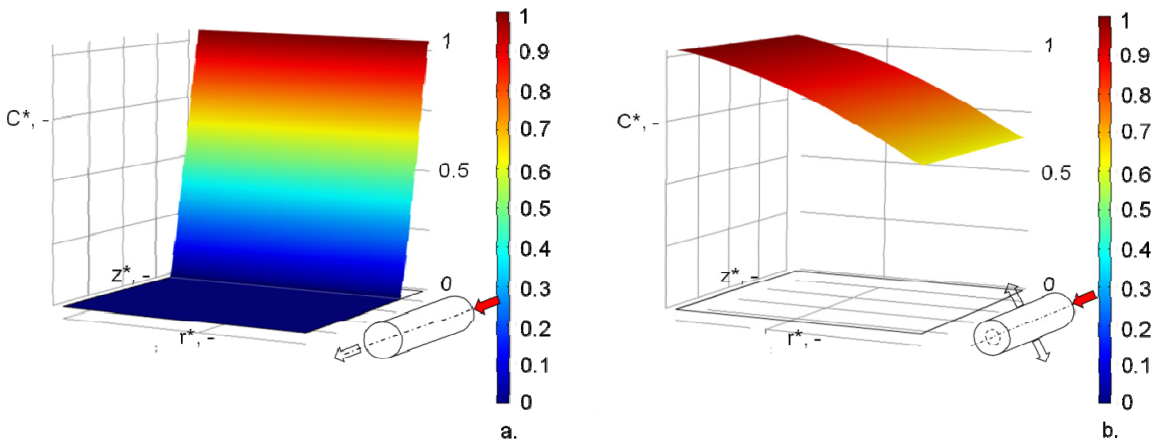

In the reports published on convection-enhanced rPBBs, it has not been paid much attention to the effect of the construct curvature on rPBB performance. In the model proposed in this paper, the construct curvature is accounted for by the ratio of the inner hollow cavity radius to the construct annular thickness, R_i/δ_C. Model-predicted dissolved oxygen concentration profiles were obtained at varying values of this dimensionless group by keeping δ_C constant and by varying the construct inner radius R_i to avoid changes of the other dimensionless groups. This way, dimensionless groups such as the $Pe_{rad,max}$ and φ_C, as well as the oxygen transport path-length and medium residence time, were kept constant. Figure 5 shows the dissolved oxygen concentration profiles across the annular wall of constructs featuring two values of R_i/δ_C an order of magnitude different, at increasing Thiele moduli. At any given R_i/δ_C, the dissolved oxygen concentration decreases in the direction of medium perfusion with a steeper slope as the Thiele modulus increases. Figure 5 shows that in constructs with greater curvature, *i.e.*, lower R_i/δ_C, increasing Thiele moduli cause a greater oxygen concentration decay along the direction of medium perfusion than in constructs with smaller curvature, *i.e.*, higher R_i/δ_C. Figure 5a shows that for $R_i/\delta_C = 0.1$ and $\varphi_C = 4$ cells are cultured under hypoxic conditions in about 32% of the construct volume. Figure 5b shows that at $R_i/\delta_C = 1$ and $\varphi_C = 4$ the dissolved oxygen concentration profile is much smoother and oxygen concentration is above 50% of the feed almost everywhere in the construct. This suggests that constructs of smaller curvature, *i.e.*, higher R_i/δ_C, may help obtain more uniform dissolved oxygen concentration profiles throughout the construct in all those applications in which the control of the pericellular environment is important (e.g., in the *in vitro* toxicity test of drugs).

Figure 5. Model-predicted dimensionless oxygen concentrations along the annular wall of constructs, cultured in an rPBB and perfused outwards with medium (*i.e.*, $\gamma = 1$), featuring different curvature: (**a**) $R_i/\delta_C = 0.1$; (**b**) $R_i/\delta_C = 1$. Other parameters as in Tables 2 and 3.

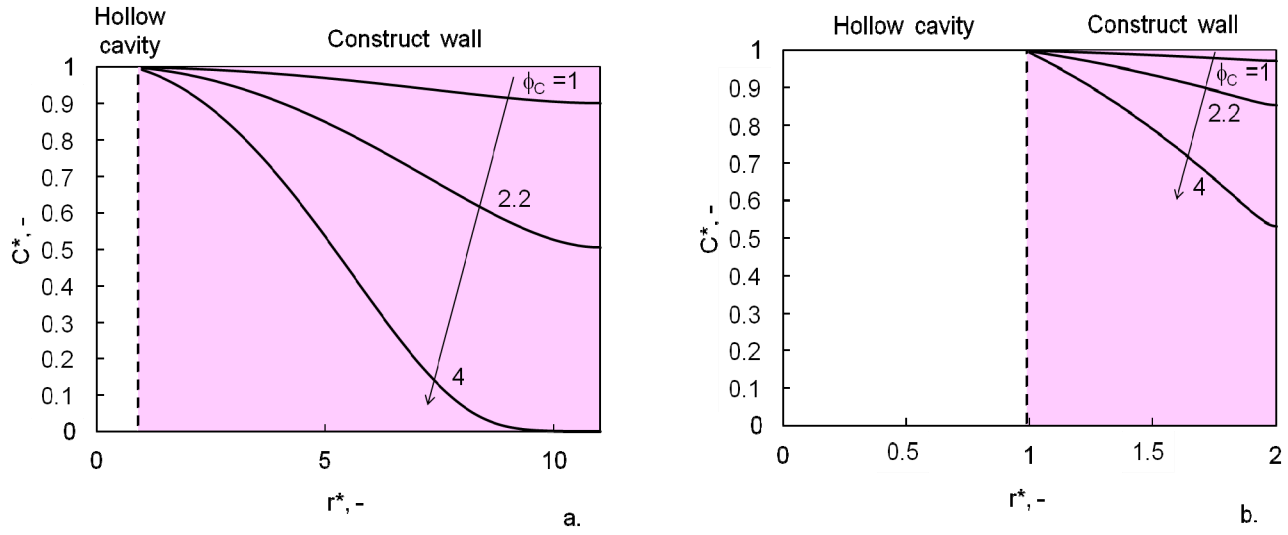

In the first decisional phases of the design of rPBBs it may be convenient to condense the bioreactor performance in one parameter only, and to analyze the influence of the most relevant dimensionless groups on this performance parameter. The basic requirement for human cell culture for therapeutic treatments (as well as for the *in vitro* drug testing) is that cells are viable and express differentiated tissue-specific functions for the duration of the treatment (or the *in vitro* test). Culturing cells at

controlled pericellular dissolved oxygen concentrations within the physiological range of the specific cell niche seems a reasonable approach to avert cell death by anoxia or by hyperoxic poisoning [65]. In this paper, the performance of the rPBB was condensed in the non-hypoxic fractional construct volume (NHy-FCV). When oxygen convective transport becomes important, the balance between the rate of physical transport and metabolic consumption is better evaluated in terms of the Damköhler number rather than the Thiele modulus. In rPBBs, the radial superficial velocity varies along the construct radius. A minimal radial Damköhler number $Da_{rad,min}$ may be defined as the ratio of the squared Thiele modulus to the maximal radial Peclet number, $Da_{rad,min} = \varphi_C^2/Pe_{rad,max}$. Figure 6 shows how the NHy-FCV varies with increasing $Da_{rad,min}$ at values of the curvature, R_i/δ_C, varying by three orders of magnitude, for both inward and outward medium perfusion. Independent of the direction of medium perfusion and R_i/δ_C, at sufficiently low $Da_{rad,min}$ the bioreactor is operated under kinetic control, *i.e.*, the dissolved oxygen concentration profile is nearly uniform in the construct, and NHy-FCV approaches unity. At high $Da_{rad,min}$ the bioreactor is operated under transport control, *i.e.*, winning the transport resistance requires significant amounts of the oxygen supplied, and NHy-FCV is lower than unity. Faster consumption rates worsen the scenario, and NHy-FCV linearly decreases with increasing $Da_{rad,min}$ in the log-log plot shown in Figure 6. Figure 6 shows that the transition between kinetic and transport control occurs at a value of $Da_{rad,min}$ which increases as the curvature of the construct decreases. At any given R_i/δ_C, the negative slope of the NHy-FCV dependence on $Da_{rad,min}$ under transport-limited conditions is lower when medium is perfused outwards across the construct. Figure 6 shows that for $Da_{rad,min} = 0.2$ and $R_i/\delta_C = 0.1$ cells are well oxygenated in about 90% of the construct volume when medium is perfused outwards, whereas the well oxygenated construct volume decreases to only about 40% when medium is perfused inwards. rPBBs in which constructs with smaller curvature are used, *i.e.*, higher R_i/δ_C, are generally more robust. In fact, inward medium perfusion or the increase of $Da_{rad,min}$ as tissue matures (e.g., cells proliferate or differentiate to a phenotype with higher metabolic requirements) causes a smaller decrease of NHy-FCV than in the radial perfusion culture of constructs with greater curvature, *i.e.*, lower R_i/δ_C. Figure 6 shows that for $Da_{rad,min} = 1$ and $R_i/\delta_C = 1$ the NHy-FCV decreases ca. 28% from 0.7 to 0.5 upon switching from outward to inward medium perfusion, respectively. At the same $Da_{rad,min}$ and for $R_i/\delta_C = 10$, the NHy-FCV is independent of the direction of medium perfusion. The smaller NHy-FCV for inward medium perfusion may be blamed on the fact that the oxygen-rich feed enters the construct through its outer surface at the minimal superficial radial velocity. Under such conditions, the cells located in the construct periphery consume oxygen at the highest metabolic rate and have time enough to deplete the medium of oxygen and establish steep dissolved oxygen concentration gradients. When medium is perfused outwards, the oxygen-rich feed enters the construct through its inner surface at the maximal radial superficial velocity. Under such conditions, the cells located in the construct close to the inner hollow cavity consume oxygen at the highest metabolic rate but are not given time enough to deplete the medium of oxygen, which will be more available to cells located in the construct periphery where medium flows at the minimal superficial radial velocity. This leads to the establishment of smoother dissolved oxygen concentration profiles along the direction of medium perfusion. The NHy-FCV dependence on the minimal radial Damköhler number $Da_{rad,min}$ shown in Figure 6 is consistent with that reported by Moustafa *et al*. [66], who showed that higher substrate conversions (*i.e.*, lower substrate concentrations) are obtained in rPBRs for industrial applications if the bed of porous inorganic catalyst

is perfused inwards when gas-phase reactions with Langmuir-Hinshelwood kinetics take place. The model-predicted effect of the direction of flow perfusion is in apparent contrast to the general use of inward perfusion in published reports on rPBBs and to Olivier *et al*. [36], who reported experiments showing that inward medium perfusion enhances osteoblastic cell proliferation to a greater extent than outward perfusion. In their paper, Olivier *et al*., raised an important practical issue influencing the decision as to whether an rPBB should be perfused with medium outwards or inwards. In fact, many cylindrical scaffolds have pores of increasing size towards their periphery [34], causing significant reduction of the local specific surface area. If cells attach weakly to the scaffold surface, for its chemical nature or for the little surface area available for adhesion, outward medium perfusion may exert high enough mechanical stresses to remove the adherent cells and wash them out. When medium is perfused inwards, the finer pores in the construct inner regions may act as a sieve and may retain the removed cells, thus avoiding cell wash-out. In addition to this, upon assuming that the MG63 osteoblastic cells used in [36] consume oxygen at 1.33×10^{-18} mol/(s cell), as other immortalized cell lines [67], and for a cell concentration of 2.8×10^{6} cell/mL, the minimal radial Damköhler number of the construct may be estimated to be about $Da_{rad,min} = 4.5 \times 10^{-4}$. Figure 6 shows that at such a low value of $Da_{rad,min}$ the rPBB is operated under kinetic control and the bioreactor performance is independent of the direction of medium perfusion. This suggests that cell wash-out may indeed have played an important role in making inward medium perfusion enhance the number of cells found in the construct after 7 and 28 days of culture to a greater extent than outward perfusion. This effect should be seriously considered when the conditions are chosen under which an rPBB is operated. Figure 6 suggests that, during cell culture in rPBBs, a low $Da_{rad,min}$ should be maintained to minimize oxygen concentration gradients across the construct. This could be achieved by perfusing thin constructs at high maximal radial superficial velocities, v_o, for as much as is permitted by cell resistance to shear damage. It suggests also that, as tissue matures, increasing v_o may balance out the increase of cell metabolic activity caused by cell proliferation and differentiation.

Figure 6. Model-predicted dependence on $Da_{rad,min}$ of the NHy-FCV of 3D porous hollow cylindrical constructs featuring varying wall curvature, R_i/δ_C, in an rPBB when radially perfused with medium outwards ($\gamma = 1$, solid lines), or inwards ($\gamma = -1$, dashed lines).

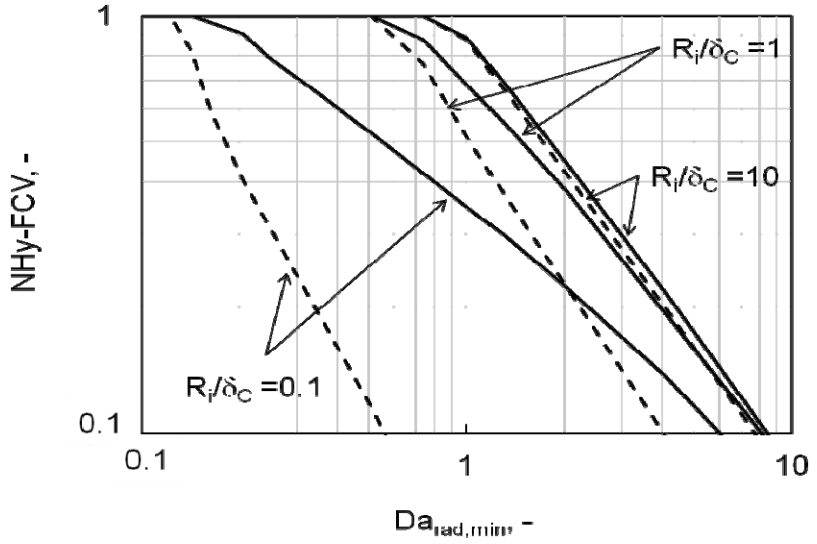

It is important to recall that model predictions are as good as the assumptions upon which the model is based. An important assumption on transport is that medium perfuses the construct at a uniform superficial velocity along its length. Axial variations of the porous structure of the scaffold may make its Darcy permeability significantly vary along the construct length and may cause superficial radial velocity maldistribution. In the use of rPBBs for human cell culture, the flow maldistribution would cause a non-uniform supply of dissolved oxygen, nutrients and biochemical cues to cells that, in time, might yield a non-uniform distribution of cells and cell activities. This way, cells would synthesize and deposit the own extracellular matrix non-uniformly in the construct worsening even further the radial flow maldistribution and its effects. Additional phenomena possibly affecting the transport and the actual concentration of larger solutes (e.g., the physical adsorption of proteins to the scaffold) have also been neglected on the account of the low molecular weight and high mobility of oxygen. With respect to cell metabolism, the model proposes a description limited to oxygen consumption and its dependence on the dissolved oxygen concentration. Work is under way to include in the model other metabolic activities and substrates relevant to given therapeutic applications, and the effects on cell metabolism of physical cues (e.g., shear stress) [68] and the accumulation of metabolic wastes (e.g., lactate). A word of caution is also in order concerning the fact that the value of condensed performance parameters such as NHy-FCV and the shape of diagrams such as that shown in Figure 6 strongly depend on the threshold value set for the dissolved oxygen concentration below which cells become apoptotic or die.

4. Conclusions

The use of radial flow packed-bed bioreactors (rPBBs) for therapeutic applications may be advantageous to overcome the typical limitations of static and axial perfusion bioreactors. In this paper, a reference model framework is proposed to help bioreactor designers optimize geometry and operation of rPBBs to meet given therapeutic requirements. The framework is based on a model in which transport across an annular cell-seeded construct is described according to the Darcy and the dispersion-convection-reaction equations. Dimensional analysis was used to combine more effectively geometric and operational variables in the dimensionless groups determining the rPBB performance. Their effect was investigated on bioreactor performance. The effectiveness of cell oxygenation was also expressed in terms of the non-hypoxic fractional construct volume (NHy-FCV), which was deemed more apt than other integral performance parameters used in technical applications. Model predictions suggest that outward radial perfusion of a 3D porous hollow cylindrical construct with small curvature (*i.e.*, high inner hollow cavity radius-to-annular thickness ratio) at high perfusion flow rates (*i.e.*, high maximal radial Peclet numbers) may be more convenient than culture in static or axial perfusion bioreactors. In fact, this would enable effective oxygenation of human cells also in large-scale constructs and culture at more controllable (e.g., more uniform) concentration profiles of dissolved oxygen and biochemical cues, at tolerable pressure drops. In conclusion, culture of human cell-seeded constructs in perfused rPBBs may permit robust control of the pericellular environment, and guidance of cell proliferation and differentiation in the engineering of biological substitutes. These features make rPBBs suitable for therapeutic treatments as well as for the *in vitro* toxicity screening of drugs. However, model predictions are as good as the assumptions upon which the model is based. In

designing an rPBB with the model proposed, care should be taken to use model parameters estimated from culture experiments and to verify that the model assumptions hold true for the specific case considered. It should also be noted that the value of integral performance parameters, such as NHy-FCV, and diagrams such as that shown in Figure 6 strongly depend on the threshold value set for the dissolved oxygen concentration below which cells become apoptotic or die.

Acknowledgments

The study was co-funded by the Italian Ministry of Instruction and University (MIUR) (Project PRIN 2010, MIND). One of the authors (DD) was financially supported by a scholarship of the European Social Fund of the European Commission, kindly assigned by the Region Calabria.

Conflicts of Interest

The authors declare no conflict of interest.

References

1. Langer, R.; Vacanti, J.P.; Vacanti, C.A.; Atala, A.; Freed, L.E.; Vunjak-Novakovic, G. Tissue engineering: Biomedical applications. *Tissue Eng*. **1995**, *1*, 151–161.
2. VandeVord, P.J.; Nasser, S.; Wooley, P.H. Immunological responses to bone soluble proteins in recipients of bone allografts. *J. Orthop. Res.* **2005**, *23*, 1059–1064.
3. Zeilinger, K.; Holland, G.; Sauer, I.M.; Efimova, E.; Kardassis, D.; Obermayer, N.; Liu, M.; Neuhaus, P.; Gerlach, J.C. Time course of primary liver cell reorganization in three-dimensional high-density bioreactors for extracorporeal liver support: An immunohistochemical and ultrastructural study. *Tissue Eng*. **2004**, *10*, 1113–1124.
4. Rotem, A.; Toner, M.; Bhatia, S.N.; Foy, B.D.; Tomkins, R.G.; Yarmush, M.L. Oxygen is a factor determining *in vitro* tissue assembly: Effects on attachment and spreading of hepatocytes. *Biotechnol. Bioeng.* **1994**, *43*, 654–660.
5. Catapano, G.; de Bartolo, L.; Lombardi, C.P.; Drioli, E. The effect of oxygen transport resistances on the viability and functions of isolated rat hepatocytes. *Int. J. Artif. Organs* **1996**, *19*, 31–41.
6. Allen, J.W.; Khetani, S.R.; Bhatia, S.N. *In vitro* zonation and toxicity in a hepatocyte bioreactor. *Toxicol. Sci*. **2005**, *84*, 110–119.
7. Volkmer, E.; Drosse, I.; Otto, S.; Stangellmayer, A.; Stengele, M.; Kallukalam, B.C.; Mutschler, W.; Schieker, M. Hypoxia in static and dynamic 3D culture systems for tissue engineering of bone. *Tissue Eng. Part A* **2008**, *14*, 1331–1340.
8. Griffith, C.K.; George, S.C. The effect of hypoxia on *in vitro* prevascularization of a thick soft tissue. *Tissue Eng. Part A* **2009**, *15*, 2423–2434.
9. Catapano, G. Mass transfer limitations to the performance of membrane bioartificial liver support devices. *Int. J. Artif. Organs* **1996**, *19*, 51–68.
10. Wendt, D.; Marsano, A.; Jakob, M.; Heberer, M.; Martin, I. Oscillating perfusion of cell suspensions through three-dimensional scaffolds enhances cell seeding efficiency and uniformity. *Biotechnol. Bioeng.* **2003**, *84*, 205–214.

11. Glicklis, R.; Shapiro, L.; Agbaria, R.; Merchuk, J.C.; Cohen, S. Hepatocyte behavior within three-dimensional porous alginate scaffolds. *Biotechnol. Bioeng.* **2000**, *67*, 344–353.
12. Gaspar, D.A.; Gomide, V.; Monteiro, F.J. The role of perfusion bioreactors in bone tissue engineering. *Biomatter* **2012**, *2*, 1–9.
13. Muschler, G.F.; Nakamoto, C.; Griffith, L. Engineering principles of clinical cell-based tissue engineering. *J. Bone Joint Surg.* **2004**, *86*, 1541–1558.
14. Griffith, C.K.; George, S.C. Diffusion limits of an *in vitro* thick prevascularized tissue. *Tissue Eng*. **2005**, *11*, 257–266.
15. Jaesung, P.; Yawen, L.; Berthiaume, F.; Toner, M.; Yarmush, M.L.; Tilles, A.W. Radial flow hepatocyte bioreactor using stacked microfabricated grooved substrates. *Biotechnol. Bioeng*. **2008**, *99*, 455–467.
16. Niu, M.; Hammond, P.; Coger, R.N. The effectiveness of a novel cartridge-based bioreactor design in supporting liver cells. *Tissue Eng. Part A* **2009**, *15*, 2903–2916.
17. Granet, C.; Laroche, N.; Vico, L.; Alexandre, C.; Lafage-Proust, M.H. Rotating wall vessel, promising bioreactors for osteoblastic cell culture: Comparison with other 3D conditions. *Med. Biol. Eng. Comput.* **1998**, *36*, 513–519.
18. Sikavitsas, V.I.; Bancroft, G.N.; Mikos, A.G. Formation of three-dimensional cell/polymer constructs for bone tissue engineering in a spinner flask and a rotating wall vessel bioreactor. *J. Biomed. Mater. Res*. **2002**, *62*, 36–48.
19. Catapano, G.; Gerlach, J.C. Bioreactors for liver tissue engineering. On-line encyclopedia of tissue engineering. In *Topics in Tissue Engineering*; Ashammakhi, N., Reis, R., Chiellini, E., Eds.; Biomaterials and Tissue Engineering Group: Oulu, Finland, 2007; Volume 3, Chapter 8, pp. 1–42. Available online: http://www.oulu.fi/spareparts/ebook_topics_in_t_e_vol3/ (accessed on 27 December 2013).
20. Radisic, M.; Deen, W.; Langer, R.; Vunjak-Novakovic, G. Mathematical model of oxygen distribution in engineered cardic tissue with parallel channel array perfused with culture medium containing oxygen carriers. *Am. J. Physiol. Heart Circ. Physiol*. **2005**, *288*, H1278–H1289.
21. Sullivan, J.P.; Palmer, A.F. Targeted oxygen delivery within hepatic hollow fiber bioreactors via supplementation of hemoglobin-based oxygen carriers. *Biotechnol. Prog*. **2006**, *22*, 1374–1387.
22. McClelland, R.E.; Coger, R.N. Use of micropathways to improve oxygen transport in a hepatic system. *Trans. ASME* **2000**, *122*, 268–273.
23. McClelland, R.E.; Coger, R.N. Effects of enhanced O_2 transport on hepatocytes packed within a bioartificial liver device. *Tissue Eng*. **2004**, *10*, 253–266.
24. Kim, S.S.; Sundback, C.A.; Kaihara, S.; Benvenuto, M.S.; Kim, B.-S.; Mooney, D.J.; Vacanti, J.P. Dynamic seeding and *in vitro* culture of hepatocytes in a flow perfusion system. *Tissue Eng*. **2000**, *6*, 39–44.
25. Bancroft, G.N.; Sikavitsas, V.I.; van der Dolder, J.; Sheffield, T.L.; Ambrose, C.G.; Jansen, J.A.; Mikos, A.G. Fluid flow increases mineralized matrix deposition in 3D perfusion culture of marrow stromal osteoblasts in a dose-dependent manner. *Proc. Natl. Acad. Sci. USA* **2002**, *99*, 12600–12605.

26. Warnock, J.N.; Bratch, K.; Al-Rubeai, M. Packed-bed bioreactors. In *Bioreactors for Tissue Engineering*, 1st ed.; Chauduri, J., Al-Rubeai, M., Eds.; Springer Verlag: Dordrecht, The Netherlands, 2005; pp. 87–114.
27. Fröhlich, M.; Grayson, W.L.; Marolt, D.; Gimble, J.M.; Kregar-Velikonja, N.; Vunjak-Novakovic, G. Bone grafts engineered from human adipose-derived stem cells in perfusion bioreactor culture. *Tissue Eng.* **2010**, *16*, 179–189.
28. Piret, J.M.; Devens, D.A.; Cooney, C.L. Nutrient and metabolite gradients in mammalian-cell hollow fiber bioreactors. *Can. J. Chem. Eng.* **1991**, *69*, 421–428.
29. Fassnacht, D.; Pörtner, R. Experimental and theoretical considerations on oxygen supply for animal cell growth in fixed-bed reactors. *J. Biotechnol.* **1999**, *72*, 169–184.
30. Singh, H.; Ang, E.S.; Lim, T.T.; Hutmacher, D.W. Flow modeling in a novel non-perfusion conical bioreactor. *Biotechnol. Bioeng*. **2007**, *97*, 1291–1299.
31. Kurosawa, H.; Markl, H.; Niebhur-Redder, C.; Matsamura, M. Dialysis bioreactor with radial flow fixed bed for animal cell culture. *J. Ferment. Bioeng*. **1991**, *72*, 41–45.
32. Kino-Oka, M.; Taya, M. Design and operation of a radial flow bioreactor for reconstruction of cultured tissues. In *Bioreactors for Tissue Engineering*, 1st ed.; Chauduri, J., Al-Rubeai, M., Eds.; Springer Verlag: Dordrecht, The Netherlands, 2005; pp. 115–133.
33. Guillouzo, A.; Guguen-Guillouzo, C. Evolving concepts in liver tissue modeling and implications for *in vitro* toxicology. *Expert Opin. Drug Metab. Toxicol*. **2008**, *4*, 1279–1294.
34. Kitagawa, T.; Yamaoka, T.; Iwase, R.; Murakami, A. Three-dimensional cell seeding and growth in radial-flow perfusion bioreactor for in vitro tissue reconstruction. *Biotechnol. Bioeng*. **2006**, *93*, 947–954.
35. Xie, Y.; Hardouin, P.; Zhu, Z.; Tang, T.; Dai, K.; Lu, J. Three-dimensional flow perfusion culture system for stem cell proliferation inside the critical-size β-tricalcium phosphate scaffold. *Tissue Eng*. **2006**, *12*, 3535–3543.
36. Olivier, V.; Hivart, P.; Descamps, M.; Hardouin, P. *In vitro* culture of large bone substitutes in a new bioreactor: Importance of the flow direction. *Biomed. Mater*. **2007**, *2*, 174–180.
37. Kawada, M.; Nagamori, S.; Aizaki, H.; Fukaya, K.; Niiya, M.; Matsuura, T.; Sujino, H.; Hasumura, S.; Yashida, H.; Mizutani, S.; *et al*. Massive culture of human liver cancer cells in a newly developed radial flow bioreactor system: Ultrafine structure of functionally enhanced hepatocarcinoma cell lines. *In Vitro Cell Dev. Biol. Anim.* **1998**, *34*, 109–115.
38. Hongo, T.; Kajikawa, M.; Ishida, S.; Ozawa, S.; Ohno, Y.; Sawada, J.; Umezawa, A.; Ishikawa, Y.; Kobayashi, T.; Honda, H. Three-dimensional high-density culture of HepG2 cells in a 5-mL radial flow bioreactor for construction of artificial liver. *J. Biosci. Bioeng*. **2005**, *99*, 237–244.
39. Miskon, A.; Sasaki, N.; Yamaoka, T.; Uyama, H.; Kodama, M. Radial flow type bioreactor for bioartificial liver assist using PTFE non-woven fabric coated with poly-amino acid urethane copolymer. *Macromol. Symp.* **2007**, *249–250*, 151–158.
40. Morsiani, E.; Galavotti, D.; Puviani, A.C.; Valieri, L.; Brogli, M.; Tosatti, S.; Pazzi, P.; Azzena, G. Radial flow bioreactor outperforms hollow-fiber modulus as a perfusing culture system for primary porcine hepatocytes. *Transplant. Proc.* **2000**, *32*, 2715–2718.

41. Morsiani, E.; Brogli, M.; Galavotti, D.; Bellini, T.; Ricci, D.; Pazzi, P.; Puviani, A.C. Long-term expression of highly differentiated functions by isolated porcine hepatocytes perfused in a radial-flow bioreactor. *Artif. Organs* **2001**, *25*, 740–748.
42. Saito, M.; Matsuura, T.; Masaki, T.; Maehashi, H.; Shimizu, K.; Hataba, Y.; Iwahori, T.; Suzuki, T.; Braet, F. Reconstruction of liver organoid using bioreactor. *World J. Gastroenterol*. **2006**, *12*, 1881–1888.
43. Ishii, Y.; Saito, R.; Marushima, H.; Ito, R.; Sakamoto, T.; Yanaga, K. Hepatic reconstruction from fetal porcine liver cells using a radial flow bioreactor. *World J. Gastroenterol.* **2008**, *14*, 2740–2747.
44. Tharakan, J.P.; Chau, P.C. Modeling and analysis of radial flow mammalian cell culture. *Biotechnol. Bioeng*. **1987**, *29*, 657–671.
45. Cima, L.G.; Blanch, H.W.; Wilke, C.R. A theoretical and experimental evaluation of a novel radial-flow hollow fiber reactor for mammalian cell culture. *Bioprocess Eng.* **1990**, *5*, 19–30.
46. Böhmann, A.; Pörtner, R.; Schmieding, J.; Kasche, V.; Markl, H. The membrane dialysis bioreactor with integrated radial-flow fixed bed—A new approach for continuous cultivation of animal cells. *Cytotechnology* **1992**, *9*, 51–57.
47. Pörtner, R.; Platas, O.B.; Fassnacht, D.; Nehring, D.; Czermak, P.; Markl, H. Fixed bed reactors for the cultivation of mammalian cells: Design, performance and scale-up. *Open Biotechnol. J.* **2007**, *1*, 41–46.
48. Chang, H.C.; Saucier, M.; Calo, J.M. Design criterion for radial flow fixed-bed reactors. *AIChE J.* **1983**, *29*, 1039–1041.
49. Delgado, J. A critical review of dispersion in packed beds. *Heat Mass Transfer* **2006**, *42*, 279–310.
50. Fogler, H.S. *Elements of Chemical Reaction Engineering*, 4th ed.; Prentice Hall: Westford, MA, USA, 2006; pp. 946–943.
51. Bird, R.B.; Stewart, W.E.; Lightfoot, E.N. *Transport Phenomena*, 2nd ed.; John Wiley & Sons, Inc.: New York, NY, USA, 2007; pp. 545–568.
52. Han, P.; Bartels, D.M. Temperature dependence of oxygen diffusion in H_2O and D_2O. *J. Phys. Chem*. **1996**, *100*, 5597–5602.
53. Abdullah, N.S.; Das, D.B.; Ye, H.; Cui, Z.F. 3-D bone tissue growth in hollow fibre membrane bioreactor: Implications of various process parameters on tissue nutrition. *Int. J. Artif. Organs* **2006**, *29*, 841–851.
54. Zahm, A.M.; Bucaro, M.A.; Ayyaswamy, P.S.; Srinivas, V.; Shapiro, I.M.; Adams, C.S.; Mukundakrishnan, K. Numerical modeling of oxygen distribution in cortical and cancellous bone: Oxygen availability governs osteonal and trabecular dimensions. *Am. J. Physiol. Cell Physiol.* **2010**, *229*, C922–C929.
55. Chen, G.; Palmer, A.F. Hemoglobin-based oxygen carrier and convection enhanced oxygen transport in a hollow fiber bioreactor. *Biotechnol. Bioeng.* **2009**, *102*, 1603–1612.
56. Loiacono, L.A.; Shapiro, D.S. Detection of hypoxia at the cellular level. *Crit. Care Clin.* **2010**, *26*, 409–421.
57. Clarke, B. Normal bone anatomy. *Clin. J. Am. Soc. Nephrol*. **2008**, *3*, S131–S139.
58. Tortora, G.J.; Derrickson, B. *Principles of Anatomy and Physiology*, 11th ed.; John Wiley & Sons, Inc.: New York, NY, USA, 2006.

59. Ponzi, P.R.; Kaye, L.A. Effect of flow maldistribution on conversion and selectivity in radial flow fixed-bed reactors. *AIChE J*. **1979**, *25*, 100–108.
60. Komarova, S.V.; Ataullakhanov, F.I.; Globus, R.K. Bioenergetics and mitochondrial transmembrane potential during differentiation of cultured osteoblasts. *Am. J. Physiol. Cell Physiol.* **2000**, *279*, C1220–C1229.
61. Balis, U.J.; Behnia, K.; Dwarakanath, B.; Bhatia, S.N.; Sullivan, S.J.; Yarmush, M.L.; Toner, M. Oxygen consumption characteristics of porcine hepatocytes. *Metab. Eng*. **1999**, *1*, 49–62.
62. Mehta, K.; Mehta, G.; Takayama, S.; Linderman, J. Quantitative inference of cellular parameters from microfluidic cell culture systems. *Biotechnol. Bioeng.* **2009**, *103*, 966–974.
63. Wang, S.; Tarbell, J.M. Effect of fluid flow on smooth muscle in a 3-dimensional collagen gel model. *Arterioscler. Thromb. Vasc. Biol*. **2000**, *20*, 2220–2225.
64. Christi, Y. Hydrodynamic damage to animal cells. *Crit. Rev. Biotechnol.* **2001**, *21*, 67–110.
65. Navdeep, S.; Chandel, G.R.; Budinger, S. The cellular basis for diverse responses to oxygen. *Free Radic. Biol. Med*. **2007**, *42*, 165–174.
66. Moustafa, T.; Badr, S.; Hassan, M.; Abba, I.A. Effect of flow direction on the behavior of radial flow catalytic reactors. *Asia-Pac. J. Chem. Eng.* **2012**, *7*, 307–316.
67. Rowley, J.A.; Timmins, M.; Galbraith, W.; Garvin, J.; Kosovsky, M.; Heidaran, M. Oxygen consumption as a predictor of growth and differentiation of MC3T3-E1 osteoblasts on 3D biodegradable scaffolds. *Mol. Biol. Cell* **2002**, *13*, 345a.
68. Kretzmer, G.; Schügerl, K. Response of mammalian cells to shear stress. *Appl. Microbiol. Biotechnol*. **1991**, *34*, 613–616.

© 2014 by the authors; licensee MDPI, Basel, Switzerland. This article is an open access article distributed under the terms and conditions of the Creative Commons Attribution license (http://creativecommons.org/licenses/by/3.0/).